Biosensors and Bioelectronics 91 (2017) 293–298

Contents lists available at ScienceDirect

Biosensors and Bioelectronics

journal homepage: www.elsevier.com/locate/bios

DNA sequence functionalized with heterogeneous core–satellite nanoassembly for novel energy-transfer-based photoelectrochemical bioanalysis

Yuan-Cheng Zhu, Fei Xu, Nan Zhang, Wei-Wei Zhao*, Jing-Juan Xu*, Hong-Yuan Chen

State Key Laboratory of Analytical Chemistry for Life Science and Collaborative Innovation Center of Chemistry for Life Science, School of Chemistry and Chemical Engineering, Nanjing University, Nanjing 210023, China

ARTICLE INFO

Keywords:
Photoelectrochemical
Bioanalysis
Ag@Au nanoparticles
Core–satellite
Energy transfer

ABSTRACT

This work reports the use of compositionally heterogeneous asymmetric Ag@Au core–satellite nanoassembly functionalized with DNA sequence as unique signaling nanoprobes for the realization of new energy-transfer-based photoelectrochemical (PEC) immunoassay of prostate- specific antigen (PSA). Specifically, the Ag@Au asymmetric core–satellite nanoassemblies (Ag@Au ACS) were fabricated on a two-dimensional glass substrate by a modified controlled assembly technique, and then functionalized with DNA sequences containing PSA aptamers as signaling nanoprobes. Then, the sandwich complexing between the PSA, its antibodies, and the signaling nanoprobes was performed on a CdS QDs modified indium tin oxide (ITO) electrode. The single stranded DNA can server as a facile mediator that place the Ag@Au ACS in proximity of CdS QDs, stimulating the interparticle exciton–plasmon interactions between Ag@Au ACS and CdS QDs and thus quenching the excitonic states in the latter. Since the damping effect is closely related to the target concentration, a novel energy-transfer-based PEC bioanalysis could be achieved for the sensitive and specific PSA assay. The developed biosensor displayed a linear range from 1.0×10^{-11} g mL^{-1} to 1.0×10^{-7} g mL^{-1} and the detection limit was experimentally found to be of 0.3×10^{-13} g mL^{-1}. This strategy used the Ag@Au ACS-DNA signaling nanoprobes and overcame the deficiency of short operating distance of the energy transfer process for feasible PEC immunoassay. More significantly, it provided a way to couple the plasmonic properties of the Ag NPs and Au NPs in a single PEC bioanalytical system. We expected this work could inspire more interests and further investigations on the advanced engineering of the core–satellite or other judiciously designed nanostructures for new PEC bioanalytical uses with novel properties.

1. Introduction

Photoelectrochemical (PEC) bioanalysis has garnered much attention in recent years for their great potential in future applications. (Gill et al., 2008; Zhang et al., 2013; Zhao et al., 2015a; Tang et al., 2015 ; Yao et al., 2013; Li et al., 2015; Long et al., 2011) For advanced PEC bioanalysis, various innovative nanoprobes that consist of specific nanomaterials functionalized with biomolecules have been utilized in plenty of rationally designed bioanalytical systems due to their significant properties. (Song et al., 2010; Xu et al., 2014) Among them, noble metal nanoparticles (Au or Ag NPs) with advantageous characteristics have been implemented in manifold applications. (Lei and Ju, 2012; Anker et al., 2008; Huang et al., 2006; Lee et al., 2006) The resonant interaction of light with the collective oscillation of free electrons in these NPs would produce the unique phenomena of surface plasmon resonance (SPR), and its generation, tuning and control has been demonstrated as a powerful route for advancing the SPR-based nanoprobes toward innovative biosensing application. (Atwater and Polman, 2010; Christopher et al., 2012; Chen et al., 2012; Da et al., 2014; Shen et al., 2014) We previously have exploited such SPR properties of Au and Ag NPs in respective PEC quantum dots (QDs) nanosystems, and different signaling mechanisms have been proposed for preliminary energy-transfer-based DNA analysis. (Zhao et al., 2011, 2012a) Such studies have aroused keen interest among the field and many recent studies were then reported sequentially. (Zeng et al., 2013; Zang et al., 2014; Zhao et al., 2015b; Fan et al., 2015; Liu et al., 2015) These increasing papers indicate intensified scientific awareness of its capabilities. However, due to its short development time, the study is still in its inception phase and there are lots of opportunities to exploit. For example, the assembly of NPs architecture

* Corresponding authors.
E-mail addresses: zww@nju.edu.cn (W.-W. Zhao), xujj@nju.edu.cn (J.-J. Xu).

http://dx.doi.org/10.1016/j.bios.2016.12.045
Received 9 October 2016; Received in revised form 12 December 2016; Accepted 17 December 2016
Available online 20 December 2016

with type, size, and/or fashion control could open great opportunities to plasmonic coupling toward specific applications. (Dey et al., 2014; Wang et al., 2012; Lakowicz, 2006; Lim and Zhong, 2009) Nevertheless, such exploitation has not been reported in the field of PEC bioanalysis.

Core–satellite nanostructure is a kind of unique NPs assembly with larger core NP surrounded by small satellite NPs, (Yoon et al., 2012, 2013; Waldeisen et al., 2011) surface plasmon coupling of the noble metal NPs could be generated from such nanostructures due to the close neighborhood between the core and the satellites. Currently, it has caused increasing interest in using the core–satellite nanostructure for bioanalytical purposes. For example, many core–satellite NPs have been utilized for the sensitive detection of chiral molecules, (Zhang et al., 2016) charge selective detection of food dyes, (Sun et al., 2016a) sensitive and reproducible DNA biosensor, (Zhang et al., 2015) ratiometric intracellular Cu^{2+} imaging, (Zou et al., 2016) and multi-modal imaging-guided combination phototherapy. (Sun et al., 2016b) In our earlier works, it was found that, Ag NPs could induce the exciton–plasmon interactions more directly and efficiently than that of Au NPs. (Zhao et al., 2011, 2012a) These novel applications of core–satellite NPs thus inspired us to construct the Ag and Au NPs-based core–satellite nanostructure for possible PEC bioanalytical uses.

Here, we report the preparation of compositionally heterogeneous asymmetric core–satellite (ACS) nanoassembly functionalized with DNA sequence as signaling nanoprobes for tentative energy-transfer-based PEC immunoassay. As demonstrated in Scheme 1A, the Ag@Au ACS were fabricated on a two-dimensional glass substrate by a modified controlled assembly technique and ultrahigh purity was obtained due to the different desorption efficiency of NPs. Using the Ag@Au ACS functionalized with DNA sequences containing protein prostate-specific antigen (PSA) aptamers, as shown in Scheme 1B, the sandwich complexing between the PSA, its antibodies, and the signaling nanoprobes was performed on a CdS QDs modified indium tin oxide (ITO) electrode. Like E-DNA sensors, the single stranded DNA can server as a facile mediator that places the Ag@Au ACS in proximity of CdS QDs, stimulating the interparticle exciton–plasmon interactions between Ag@Au ACS and CdS QDs and thus quenching the excitonic states in the latter. The damping effect is closely related to the target concentration, and thereby a novel energy-transfer-based PEC bioanalysis could be achieved for the sensitive and specific PSA assay. This strategy integrated both the plasmonic signaling mechanisms of the Ag NPs and Au NPs in a single system and overcame the deficiency of short operating distance of the energy transfer process for feasible protein immunoassay application. We expected this preliminary work could inspire more interests and further investigations on the advanced engineering of the core–satellite or other judiciously designed nanostructures for new PEC bioanalytical uses with novel properties.

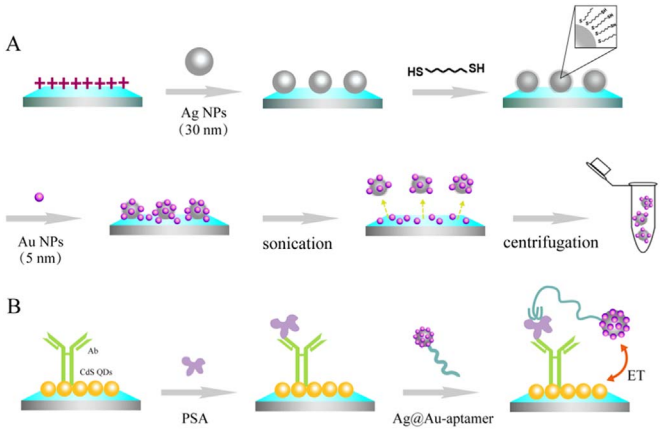

Scheme 1. The fabrication of the Ag@Au ACS for proposed PEC bioanalysis.

2. Experimental section

2.1. Materials and apparatus

Prostate specific antigen (PSA), the PSA polyclonal antibody from mouse were purchased from Shanghai Linc-Bio Science Co. Ltd. Bovine serum albumin (BSA) was obtained from Shanghai KeyGenBiotechCo., Ltd. The ITO slices (type N-STN-S1-10, China Southern Glass Holding Co., Ltd.) were used as the working electrode. The CITOGLAS positively charge glass (7.6 cm×2.6 cm) were purchased from Jiangsu Shi-Tai experimental equipment Co., Ltd. $CdCl_2{\cdot}2.5H_2O$ was obtained from Shanghai Jinshan Tingxin Chemical. Rchloroauric acid ($HAuCl_4$) was purchased from Nanjing Reagent Company (Nanjing, China). $NaBH_4$ was purchased from Tianjin Chemical Reagent Institude. $Na_2S{\cdot}9H_2O$ was obtained from Shanghai Lingfeng Chemical Reagent Co., LTD (Shanghai, China). Tris (2-carboxyethyl) phosphine hydrochloride(TCEP), PDDA (20%, w/w in water, molecular weight (200000–350000)), 1,8-octanedithiol, N-Hydroxysuccinimide(NHS), 1-Ethyl-3-(3-dimethylaminopropyl) carbodiimide (EDC) were obtained from Sigma-Aldrich. Ascorbic acid (AA), thioglycolic acid (TGA) were purchased from Sinopharm Chemical Reagent Co., Ltd (Shanghai, China). $AgNO_3$ was obtained from Shanghai Aladdin Co., Ltd. All the synthetic oligonucleotides were purchased from GenScript (Nanjing) Biological Technology Co., Ltd and the corresponding sequence was : 5′-ATT AAA GCT CGC CAT CAA ATA GCT GCT TTT TTT TTT TTT TTT T-SH-3′. All other reagents were analytical grade and were used as received. All aqueous solutions including phosphate buffer solution (PBS) were prepared using ultra-pure water (Milli-Q, Millipore). A solution of 0.01 M PBS (pH 7.4) was used to dilute the stock solution when needed. The washing buffer solution was 0.01 M PBS (pH 7.4) containing 0.05% Tween 20. The blocking buffer was 0.01 M PBS (pH 7.4) containing 3% (w/v) bull serum albumin (BSA). All aqueous solutions were prepared using ultrapure water (Milli-Q, Millipore).

PEC measurements were performed with a homemade PEC system and photocurrent was measured on a CHI 750a electrochemical workstation (China) with a three-electrode system: a modified ITO electrode with a geometrical circular area (diameter of 0.5 cm) as the working electrode, a Pt wire as the counter electrode, and a saturated Ag/AgCl electrode as the reference electrode. All the photocurrent measurements were performed at a constant potential of 0 V (versus Ag/AgCl). A 0.1 M PBS containing 0.1 M AA was used as the blank solution for photocurrent measurements. Transmission electron microscopy (TEM) was performed with a JEOL model 2000 instrument operating at 200 kV accelerating voltage. The UV–Vis absorption spectra were obtained on a Shimadzu UV-3600 UV–Vis–NIR photospectrometer (Shimadzu Co).

2.2. Synthesis of Ag NPs and Au NPs

The synthesis of Ag NPs was adopted from a previous method. (Steinigeweg and Schlücker, 2012) Firstly, 50 mL water/glycerol (40 vol% glycerol) in a 100 mL flask was heated to 95 °C under stirring (1200 rpm). Then, 9 mg silver nitrate was added. After 1 min, 1 mL (3%) sodium citrate was inject into the solution and heated at 95 °C for 1 h。 Finally , the solution was stored in a refrigerator at 4 °C for further use. Au NPs with average diameter 5 ± 1 nm were prepared through the reduction of $HAuCl_4$ by sodium $NaBH_4$. Briefly, 0.6 mL of 0.1 M ice cold $NaBH_4$ was added to 20 mL of aqueous solution containing 2.5×10^{-4} M $HAuCl_4$ under stirring, and the solution immediately turned to an orange-red color, indicating the formation of Au NPs. Then the solution was kept under stirring in the ice bath for 10 min and for another 3 h at room temperature with the color changing from orange-red to wine red. The nearly monodispersed Au NPs had an average diameter of 5 ± 1 nm as characterized by TEM and thus the final concentration of the Au colloid solution was estimated to be 6×10^{-8} M. The prepared Au NPs were kept in a refrigerator at 4 °C

for further use.

2.3. Synthesis of Ag@Au ACS and Ag@Au ACS-DNA

The synthesis of Ag@Au ACS has referred to previous work about the synthesis of Au@Au countpart. (Yoon et al., 2012) Before we begin, the glycerin in the synthesized Ag NPs solution was removed by centrifugation and the precipitation was dissolved in the water. The Ag NPs were adsorbed onto the clean positively charged glass by covering the substrate with the aqueous Ag NPs at room temperature for 8 h. The unbound Ag NPs were removed by washing with water. The surface of the adsorbed Ag NPs were functionalized with thiol groups to attach the satellite Au NPs. Immersion of the core adsorbed glass substrate in a 1, 8-octanedithiol/ethanol solution (1.0×10^{-4} M) for 12 h resulted in the formation of octanedithiol self-assembled monolayers (SAMs) on the surface of the core Ag NPs. The substrate was washed by ethanol and water sequentially. The small Au NPs were attached to the thiol-functionalized core Ag NPs on the substrate by covering the glass with Au NPs for 24 h. After washing with water, the glass was sonicated in water. Upon sonication, the core-satellite desorbed from the glass into the water. For the preparation of Ag@Au ACS labeled DNA, 50 μL of 10 μM HS-modified DNA and 10 μL of 10 mM TCEP were mixed and incubated for 1 h at 37 °C in order to reduce disulfide bonds. Then 1 mL of Ag@Au ACS solution was added into the above solution and which was incubated for 24 h at room temperature under gentle shaking and dark environment. Within the above incubation step, 200 μL of 0.5 M NaCl was smoothly added into the solution. The resultant solution was centrifuged for 10 min at 8000 rpm and 4 °C with 30 kDa Millipore. The recovered solution was kept in a refrigerator at 4 °C for further use.

2.4. Immunoassay development

The CdS QDs electrodes were fabricated using previous technique (Ma et al., 2016). Immobilization of the antibody to the CdS QDs modified electrodes was accomplished via the commonly used EDC coupling reactions between COOH groups on the surface of CdS QDs and the NH_2 groups of antibody. The CdS QDs modified electrodes were immersed in a solution containing 20 mg/mL EDC and 10 mg/mL NHS for 60 min at room temperature. After rinsing, 25 μL 0.2 mg/mL antibody was spread onto the electrode surface at 4 °C in a moisture atmosphere to avoid evaporation of solvent for 16 h, followed by thoroughly rinsing with washing buffer. The electrode was then blocked with 25 μL blocking buffer for 2 h at 4 °C to block non-specific binding sites and washed with the washing buffer thoroughly. Thus the immunoassay electrode was built. 25 μL PSA with different concentrations were dropped onto the electrodes for an incubation of 60 min at 37 °C followed by washing with washing buffer. Next, 25 μL synthesized Ag@Au-DNA were dropped onto the electrodes for an incubation of 60 min at 37 °C followed by washing with washing buffer. Finally, PEC measurements were performed on these assembled electrodes at room temperature.

3. Results and discussion

3.1. Characterization of Ag@Au ACS

Experimentally, Ag@Au ACS with a 30 nm core Ag NP decorated by 5 nm satellite Au NPs was fabricated on a positive charged glass slide by sequential adsorption of Ag and Au NPs and then following by a desorption and centrifugation procedure. The color change of the glass substrate during this synthetic process was recorded as shown in Fig. 1. The bare glass slide is transparent. After Ag NPs incubation, the color of the glass substrates turns yellow and further turns red after adsorption of Au NPs, which was attributed to the SPR of Au NPs at ca. 520 nm and indicated that Au NPs were distributed on the surfaces of the glass substrate.

The structural and optical properties of the prepared Ag NPs, Au NPs and Ag@Au ACS were characterized by transmission electron microscope (TEM) and UV–Vis spectra. As shown in Fig. 2A-B, both of the Ag NPs and Au NPs appeared as quasi-spherical particles with the sizes corresponding to 30 ± 3 nm and 5 ± 1 nm, respectively, while Fig. 2C revealed the unique features of the as-obtained Ag@Au ACS consisted a Ag NP at the core and Au NPs surrounding the core, which confirmed the feasibility of the proposed technique for fabricating Ag@Au ACS. Fig. 2D-F demonstrated the corresponding absorption spectra of these NPs. As shown, the spectra of the Ag NPs and Au NPs were clearly characterized by the maximum plasmon absorption peaks at ca. 400 nm and ca. 520 nm, respectively. Comparing with those of individual Ag NPs and Au NPs, the absorption spectra of the Ag@Au ACS exhibited the coupled surface plasmon band with two peaks, both of which were red-shifted from respective component bands. The insets in Fig. 2D-F displayed that the solution of the Ag@Au ACS appeared grayer as compared to the yellow color of the Ag NPs and the red color of Au NPs solutions.

3.2. The immunoassay development and analytical performance

The as-obtained Ag@Au ACS was then functionalized with DNA sequence for fabricating the signaling nanoprobes, and the process of which were followed by the spectra characterization. As shown in Fig. 3A, the spectra of the Ag@Au ACS-DNA nanoprobes (curve a) comprised the characteristic peak of DNA at ca. 260 nm (curve b) and that of the Ag@Au ACS (curve c), indicating the successful functionalization. On the other hand, the curve d and e corresponded to the typical absorption and photoluminescence spectrum of the CdS QDs that was used to modify the ITO glass. Obviously, the absorption spectra of Ag@Au ACS overlapped greatly with the emission spectra of the CdS QDs, indicating the simultaneous direct and indirect inducement of the exciton and plasmon in a properly designed PEC nanosystem (Zhao et al., 2011, 2012a) and thus the possibility of using such unique nanoprobes for the novel energy-transfer-based bioanalytical applications. Incidentally, the absorption spectra of Ag@Au ACS comprised the typical plasmon peaks of Ag NPs (ca. 400 nm, not shown) and a broad absorption range over 500 nm covering the plasmon absorption of Au NPs (ca. 520 nm, not shown), indicating the plasmon hybridization of the two NPs originated from the formation of Ag@Au ACS.

The system was then employed for the proposed PEC immunoassay of PSA, a serine protease that could be over expressed in prostate cancer. Fig. 3B recorded the measured chronoamperometric I–t curves from the transient photocurrent responses of the system upon the intermittent visible light illumination during the immunoassay development. As shown, the Ab immobilization and blocking as well as the capture of PSA led to a stepwise signal decrease. When Ag@Au ACS-DNA nanoprobes bound to the PSA due to the high specificity of the aptamer, the signal exhibited a notable decrease which could be attributed to the interparticle exciton–plasmon interactions between Ag@Au ACS and CdS QDs, the phenomenon of which implied the feasibility of the proposed immunoassay system. Comparing with our earlier work of catalytic Ag deposition on the Au NPs that could only stimulating the effect of Ag NPs, (Ma et al., 2016) one significant advantage of Ag@Au ACS was that it provides a way to couple the plasmonic properties of the Ag NPs and Au NPs in a single energy-transfer-based PEC bioanalytical system. In control, we compared the Ag@Au ACS with the as-prepared individual Au and Ag NPs. It turned out that the Ag NPs exhibited the strongest damping effect while the Au NPs the lowest, which indicated the predominated role of the Ag NPs in the Ag@Au ACS. The influence of the proportion of Ag and Au of ACS was further investigated, and the experimental results demonstrated that no obvious difference was existed among these Ag@Au ACS tracers. This should be attributed to the large size and the predominant

Fig. 1. The color change of the glass substrate during the synthetic process. (For interpretation of the references to color in this figure, the reader is referred to the web version of this article.)

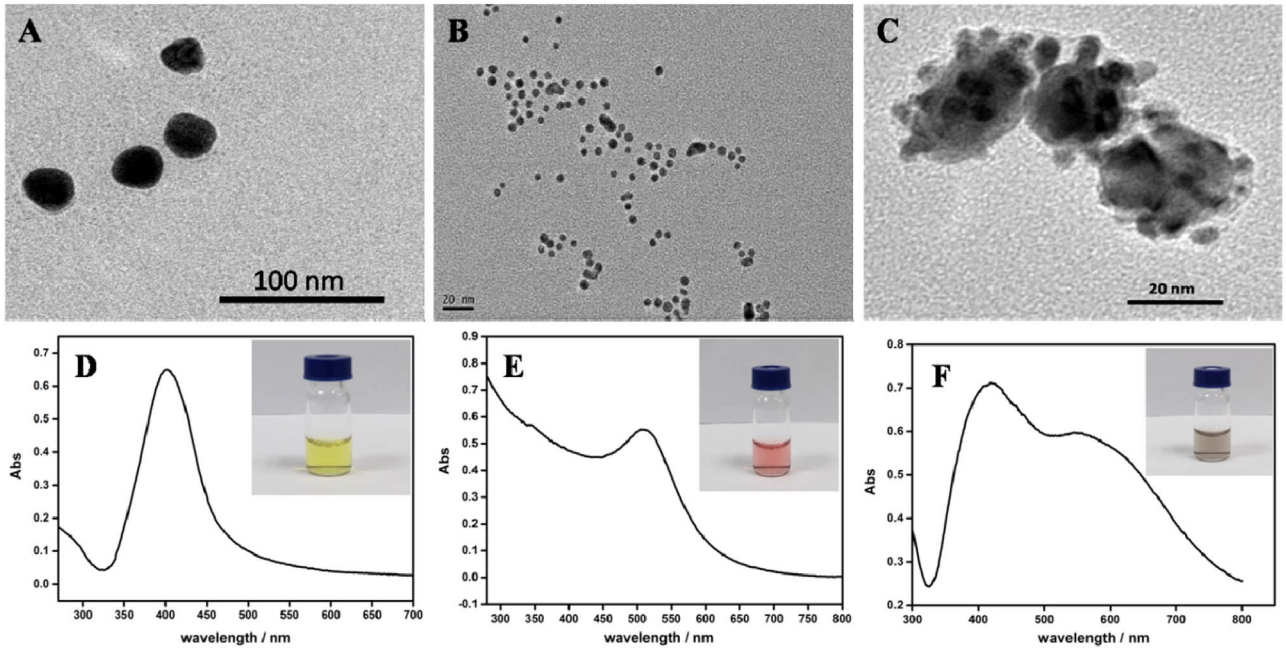

Fig. 2. (A-C) TEM and (D-F) The corresponding UV–vis spectra and the solution colors (inset) of the as-prepared Ag NPs, Au NPs and Ag@Au ACS.

damping effect of Ag NPs against the size and effect of Au NPs in current system.

Because the signal variation relates intimately with the PSA concentration, a novel PEC immunoassay can be achieved. Fig. 4A displayed the derived calibration curve of photocurrent responding after incubation with increased PSA concentrations. As demonstrated, the photocurrent intensity decreased with the enhanced PSA concentration from 1.0×10^{-11} g mL^{-1} to 1.0×10^{-7} g mL^{-1}, suggesting the PSA-controlled binding of the nanoprobes. The PSA was detected with a limit of 0.3×10^{-13} g mL^{-1}, which was comparable to some recent reports of PEC PSA assays. The results were summarized in Table 1. In addition, an interassay relative standard deviation (RSD) was used to assess the reproducibility of this assay by detecting 1.0×10^{-9} g mL^{-1} samples with five electrodes, and RSD of 9.3% was obtained. The selectivity of this assay was further studied by testing 1.0×10^{-10} g mL^{-1} PSA at the presence of interfering proteins of p53, C-reactive protein

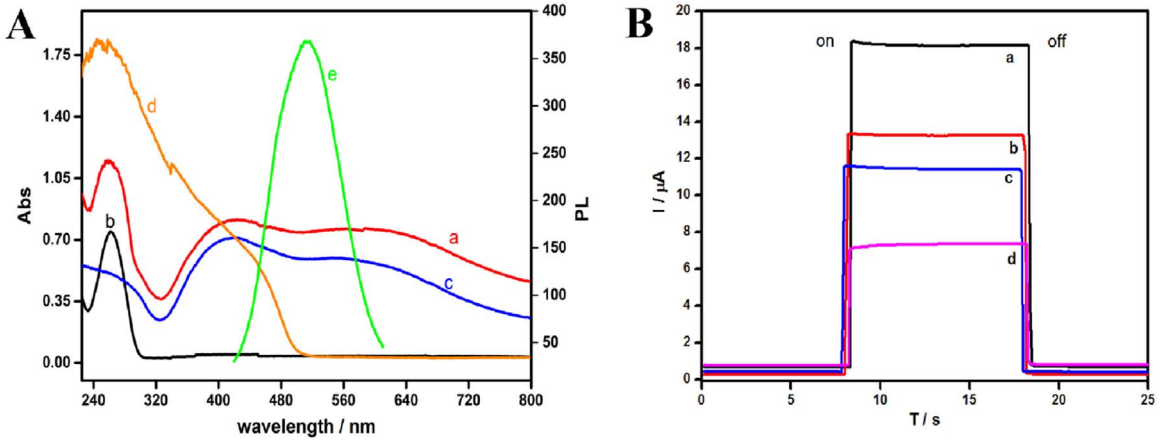

Fig. 3. (A) The absorption spectra of (a) the Ag@Au ACS-DNA nanoprobes, (b) the bare DNA, (c) the Ag@Au ACS, (d) the CdS QDs and (e) the photoluminescence spectrum of the CdS QDs. (B) Photocurrent response of (a) the developed CdS QDs electrode and after (b) the Ab immobilization and blocking, (c) capture the target at the concentration of 1.0×10^{-7} g mL^{-1}, and (d) the recognition of Ag@Au ACS-DNA nanoprobes. The tests were performed in 0.1 M PBS solution containing 0.1 M AA with a constant potential of 0.0 V.

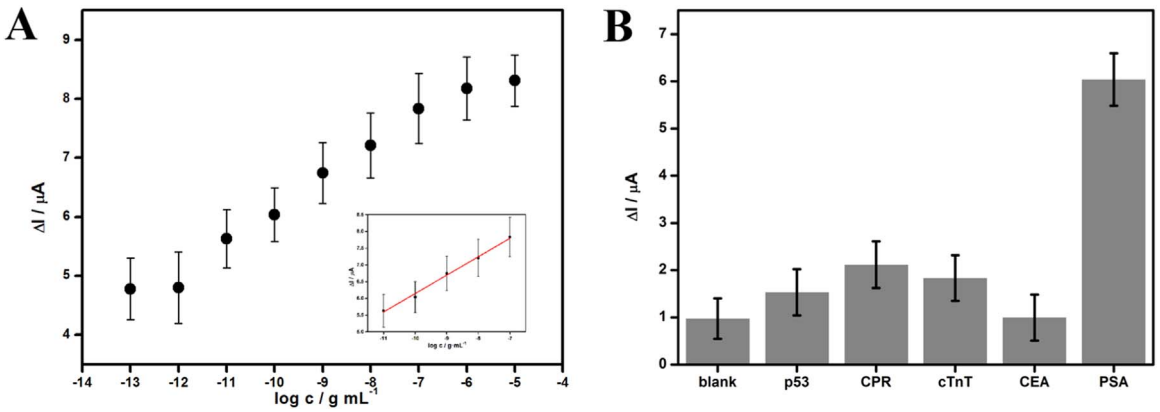

Fig. 4. (A) Plot of the photocurrent vs PSA concentration. Inset: the derived calibration curve. (B) Selectivity of the proposed immunoassay to PSA by comparing it to the interfering proteins of p53, CRP, cTnT and CEA. ΔI was the photocurrent decrement corresponding to variable PSA concentration. The tests were performed in 0.1 M PBS solution containing 0.1 M AA with a constant potential of 0.0 V.

Table 1
Comparison of the analytical performance of some recent PEC PSA assays.

Detection method	Linear range (g mL^{-1})	LOD (g mL^{-1})	References
In situ generation of electron donor	–	5.0×10^{-10}	Zhao et al. (2012b)
Chemiluminescence excited paper-based strategy	5.0×10^{-12}–1.5×10^{-7}	2.3×10^{-12}	Sun et al. (2014)
CuO-induced signal amplification strategy	1.0×10^{-12}–5.0×10^{-8}	3.0×10^{-13}	Sun et al. (2015)
Enzymatic oxydate-triggered self-illuminated strategy	1.0×10^{-11}–8.0×10^{-8}	3.0×10^{-12}	Shu et al. (2016)
Ag@Au ACS-DNA signaling nanoprobes	1.0×10^{-11}–1.0×10^{-7}	3.0×10^{-14}	This work

(CRP), troponin T (cTnT) and carcino embryonie antigen (CEA) at the same concentrations of 1.0×10^{-8} g mL^{-1}. Fig. 4B showed that the interfering proteins could not cause obvious signal reduction and hence the good selectivity. The feasibility of the immunoassay system for clinical application was investigated by adding PSA to real sample of normal human serum. The serum sample was diluted to specific concentration with a PBS of 7.4, and the recovery of 1.0×10^{-8} g mL^{-1} PSA was determined with the result of 93.1%, indicating the applicability of the proposed system for future clinical diagnosis development.

4. Conclusion

In conclusion, we have fabricated the compositionally heterogeneous Ag@Au ACS functionalized with DNA sequence and applied it for the tentative energy-transfer-based PEC immunoassay in a model system. The Ag@Au ACS could be obtained with ultrahigh purity due to the different desorption efficiency of NPs, and the single stranded DNA can server as a facile mediator that place the Ag@Au ACS near the CdS QDs electrode surface. After the sandwich complexing between the target, its antibodies, and the signaling nanoprobes, the interparticle exciton–plasmon interactions between Ag@Au ACS and CdS QDs would lead to the photocurrent quenching and thus an advanced PEC immunoassay. For the first time, this work used the Ag@Au ACS-DNA signaling nanoprobes and overcame the deficiency of short operating distance of the energy transfer process for feasible PEC immunoassay. It combined both the plasmonic properties and signaling mechanisms of the Ag NPs and Au NPs in a single energy-transfer-based PEC bioanalytical system, and the proposed format could serve as a general basis for PEC bioanalysis. By varying the core-satellite structure, constituting NPs, the core-to-satellite gap distance and the numbers of satellites, different SPR properties might be attained for advanced PEC bioanalysis. More significantly, such novel signaling nanoprobes could be expected to open more opportunities for further applications. For example, if Ab were directly bound with the tracers of Ag@Au ACS, more convenient competition assay format may be developed for specific analytical purposes.

Acknowledgements

Financial support from the National Natural Science Foundation of China (Grant nos. 21327902, 21135003, 21305063 and 21675080), and the Natural Science Funds of Jiangsu Province (Grant BK20130553) is appreciated. This work was also supported by a Project Funded by the Priority Academic Program Development of Jiangsu Higher Education Institutions.

References

Anker, J.N., Hall, W.P., Lyandres, O., Shah, N.C., Zhao, J., Duyne, R.P.V., 2008. Nat. Mater. 7, 442.
Atwater, H.A., Polman, A., 2010. Nat. Mater. 9, 865.
Chen, G., Wang, J., Wu, C., Li, C.Z., Jiang, H., Wang, X., 2012. Langmuir 28, 12393.
Christopher, P., Xin, H., Marimuthu, A., Linic, S., 2012. Nat. Mater. 11, 1044.
Da, P., Li, W., Lin, X., Wang, Y., Tang, J., Zheng, G., 2014. Anal. Chem. 86, 6633.
Dey, P., Zhu, S.L., Thurecht, K.J., Fredericks, P.M., Blakey, I., 2014. J. Mater. Chem. B 2, 2827.
Fan, G.C., Zhu, H., Shen, Q., Han, L., Zhao, M., Zhang, J.R., Zhu, J.J., 2015. Chem. Commun. 51, 7023.
Gill, R., Zayats, M., Willner, I., 2008. Angew. Chem. Int. Ed. 47, 7602.
Huang, X.H., El-Sayed, I.H., Qian, W., El-Sayed, M.A., 2006. J. Am. Chem. Soc. 128, 2115.
Lakowicz, J.R., 2006. Plasmonics 1, 5.
Lee, K.S., El-Sayed, M.A., 2006. J. Phys. Chem. B 110, 19220.
Lei, J.P., Ju, H.X., 2012. Chem. Soc. Rev. 41, 2122.
Li, C.X., Wang, H.Y., Shen, J., Tang, B., 2015. Anal. Chem. 87, 4283.
Lim, S.I., Zhong, C.J., 2009. Acc. Chem. Res. 42, 798.
Liu, S.S., Cao, H.J., Wang, Z.Y., Tu, W.W., Dai, Z.H., 2015. Chem. Commun. 51, 14259.
Long, Y.T., Kong, C., Li, D.W., Li, Y., Chowdhury, S., Tian, H., 2011. Small 7, 1624.
Ma, Z.Y., Xu, F., Qin, Y., Zhao, W.W., Xu, J.J., Chen, H.Y., 2016. Anal. Chem. 88, 4183.
Shen, Q., Jang, J., Liu, S., Han, L., Fan, X., Fan, M., Fan, Q., Wang, L., Huang, W., 2014. Nanoscale 6, 6315.
Shu, J., Qiu, Z.L., Zhou, Q., Lin, Y.X., Lu, M.H., Tang, D.P., 2016. Anal. Chem. 88, 2958.
Song, S.P., Qin, Y., He, Y., Huang, Q., Fan, C.H., Chen, H.Y., 2010. Chem. Soc. Rev. 39, 4234.
Steinigeweg, D., Schlücker, S., 2012. Chem. Commun. 48, 8682.
Sun, G.Q., Zhang, Y., Kong, Q.K., Ma, C., Yu, J.H., Ge, S.G., 2014. J. Mater. Chem. B 2, 7679.
Sun, G.Q., Zhang, Y., Kong, Q.K., Zheng, X.X., Yu, J.H., Song, X.R., 2015. Biosens. Bioelecton. 66, 565.
Sun, M., Xu, L., Ma, W., Wu, X., Kuang, H., Wang, L., Xu, C., 2016b. Adv. Mater. 28, 898.
Sun, Z., Du, J., Yan, L., Chen, S., Yang, Z., Jing, C., 2016a. ACS Appl. Mater. Interfaces 8, 3056.
Tang, J., Li, J., Da, P.M., Wang, Y.C., Zheng, G.F., 2015. Chem. Eur. J. 21, 11288.
Waldeisen, J.R., Wang, T., Ross, B.M., Lee, L.P., 2011. ACS Nano 5, 5383.
Wang, L.B., Xu, L.G., Kuang, H., Xu, C.L., Kotov, N.A., 2012. Acc. Chem. Res. 45, 1916.
Xu, J.J., Zhao, W.W., Song, S.P., Fan, C.H., Chen, H.Y., 2014. Chem. Soc. Rev. 43, 1601.
Yao, W.J., Le Goff, A., Spinelli, N., Holzinger, M., Diao, G.W., Shan, D., Defrancq, E.,

Cosnier, S., 2013. Biosens. Bioelectron. 42, 556.
Yoon, J.H., Lim, J.H., Yoon, S.W., 2012. ACS Nano 6, 7199.
Yoon, J.H., Zhou, Y., Blaber, M.G., Schatz, G.C., Yoon, S.W., 2013. J. Phys. Chem. Lett. 4, 1371.
Zang, Y., Lei, J.P., Hao, Q., Ju, H.X., 2014. ACS Appl. Mater. Interfaces 6, 15991.
Zeng, X.X., Ma, S.S., Bao, J.C., Tu, W.W., Dai, Z.H., 2013. Anal. Chem. 85, 11720.
Zhang, T., Li, H., Hou, S., Dong, Y., Pang, G., Zhang, Y., 2015. ACS Appl. Mater. Interfaces 7, 27131.
Zhang, X.R., Guo, Y.S., Liu, M.S., Zhang, S.S., 2013. RSC Adv. 3, 2846.
Zhang, Y., Liu, J., Li, D., Dai, X., Yan, F., Conlan, X.A., Zhou, R.H., Barrow, C.J., He, J., Wang, X., Yang, W., 2016. ACS Nano 10, 5096.
Zhao, M., Fan, G.C., Chen, J.J., Shi, J.J., Zhu, J., 2015b. J. Anal. Chem. 87, 12340.
Zhao, W.W., Xu, J.J., Chen, H.Y., 2015a. Chem. Soc. Rev. 44, 729.
Zhao, W.W., Wang, J., Xu, J.J., Chen, H.Y., 2011. Chem. Commun. 47, 10990.
Zhao, W.W., Ma, Z.Y., Yan, D.Y., Xu, J.J., Chen, H.Y., 2012a. Anal. Chem. 84, 10518.
Zhao, W.W., Yu, P.P., Shan, Y., Wang, J., Xu, J.J., Chen, H.Y., 2012b. Anal. Chem. 84, 5892.
Zou, C., Foda, M.F., Tan, X., Shao, K., Wu, L., Lu, Z., Bahlol, H.S., Han, H., 2016. Anal. Chem. 88, 7395.